Atom-atom correlations in spontaneous four wave mixing of two colliding Bose-Einstein Condensates

A. Perrin, H. Chang, Valentina Krachmalnicoff, M. Schellekens, D. Boiron, Alain Aspect, Christoph I Westbrook

Atom-atom correlations in spontaneous four wave mixing of two colliding Bose-Einstein Condensates

A. Perrin, H. Chang, V. Krachmalnicoff, M. Schellekens, D. Boiron, A. Aspect and C. I. Westbrook*
Laboratoire Charles Fabry de l'Institut d'Optique, CNRS, Univ Paris-Sud
Campus Polytechnique, RD128, 91127 Palaiseau cedex
(Dated: April 23, 2007)

We have used a position sensitive, single atom detector to observe atom scattering during the collision of two Bose-Einstein condensates. The process can also be thought of as spontaneous, degenerate four wave mixing of deBroglie waves. The observed two-particle correlation function shows a clear peak corresponding to the production of back to back atom pairs. The correlation function also exhibits a peak corresponding to pairs of atoms emitted in the same direction, the Hanbury Brown-Twiss effect. Our experiment is in the regime of well separated atom pairs, opening the route to the study of quantum atom optics effects with individual entangled pairs.

PACS numbers: 34.50.-s, 03.75.Nt

Recent years have seen the emergence of "quantum atom optics", that is the extension of the many analogies between atom optics and traditional optics to the quantum optical domain in which phenomena like vacuum fluctuations and entanglement play a central role. In optics the advent of correlated photon pairs [1] has provided a fruitful avenue of investigation, with examples of squeezing, single photon sources and entangled states [2]. Partly inspired by this work, there have been many proposals concerning atom pairs, especially the production and observation of entangled states [3–6] but also of squeezing [7]. Many authors have also theoretically investigated other aspects of the pair production mechanism in both atomic collisions and in the breakup of diatomic molecules [7–13].

As emphasized in Ref. [4], pair production can be studied in two limits. If many atoms are created in a single mode, stimulated emission of atoms is important and one speaks of two mode squeezing in analogy with Ref. [14]. Experiments on stimulated four wave mixing [15–17] and on parametric amplification in an optical lattice [18, 19] are in this limit. The opposite limit, in which the occupation number of the modes is much less than unity, corresponds to the spontaneous production of individual, entangled atom pairs as in [20, 21]. Atom optical experiments in this regime include the many experiments which have investigated the scattered halo in collisions of cold atoms either in the s-wave regime [22, 23] or for higher partial waves [24, 25]. To date however, the only direct observation of correlated pairs is that of Ref. [26], which showed a clear correlation signal in absorption images of atoms from the breakup of molecules near a Feshbach resonance.

In this paper we will show that the spontaneous four wave mixing process in the collision of two condensates produces individual atom pairs, and that simple coherence considerations provide a good starting point for quantitatively accounting for the observations. We also observe correlations for atoms with *collinear* velocities.

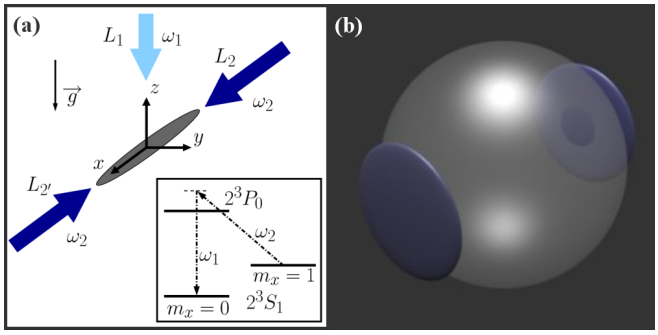

FIG. 1: (Color online) (a) View of the magnetically trapped condensate (in the $m_x = 1$ state) and the three laser beams which create two counterpropagating free condensates (in the $m_x = 0$ state) by σ^-/π Raman transfers induced by $L_1 - L_2$ and $L_1 - L_2'$ respectively (see inset). L_1 is π-polarized while L_2 and L_2' are σ^--polarized. The laser beams are blue-detuned by 400 MHz from the $2^3S_1 - 2^3P_0$ transition. The Zeeman shift between $m_x = 0$ and $m_x = 1$ is approximately 700 kHz. (b) View of the atomic density after a long enough time of flight. The scattered atoms are on the s-wave scattering sphere and the remaining, pancake-shaped condensates lie on the edge of the sphere along the x axis.

This peak was predicted in Refs. [7, 11, 12], and is another manifestation of the Hanbury Brown-Twiss effect (HBT) for an incoherent source of indistinguishable bosons, in agreement with the picture of multimode spontaneous scattering. This effect is also well known in high energy collisions [27]. Our data should provide a testing ground for more sophisticated treatments [9, 12].

An important technical innovation in this experiment is the use of a position sensitive, single atom detector which permits the measurement of the 3 dimensional velocity vectors of individual atoms. Thus rather than observing a two dimensional projection of the scattering sphere [22, 23] we reconstruct the sphere in three dimensions. In addition, and as in Refs. [28, 29], we can obtain the two-particle correlation function $g^{(2)}$, which we will

use here to identify pairs of atoms with opposite and collinear velocities.

We produce condensates of $10^4 - 10^5$ atoms in the $m_x = 1$ sublevel of the 2^3S_1 state of metastable helium (He*) [30]. The condensates are stored in a cylindrically symmetric magnetic trap with an axial trapping frequency of 47 Hz, and a radial one of 1150 Hz. The bias field is 0.25 G in the x direction (see Fig. 1), and defines the quantization axis. The detector described below measures atomic velocities. Thus an important scale for the scattered atoms is $v^{\rm rms} = \hbar/(ms)$, the velocity imposed by the uncertainty principle and the characteristic size s of the sample. The Fourier transform of the density profile for 3×10^4 atoms found by numerical calculation gives $v_{yz}^{\rm rms} = 0.091\, v_{\rm rec}$ and $v_x^{\rm rms} = 0.0044\, v_{\rm rec}$, where $v_{\rm rec} = 9.2$ cm/s is the single photon recoil velocity.

To generate two colliding Bose-Einstein condensates, three phase coherent laser beams are used to drive a stimulated Raman transition, as shown in Fig. 1. These beams have two purposes : first they transfer atoms to a magnetic field insensitive state so that they may freely fall to the detector and second, they separate the condensate into two components with velocities $v_{\rm rec}(\mathbf{e_1} \pm \mathbf{e_2})$, where $\mathbf{e_1}$ and $\mathbf{e_2}$ are respectively the unit vectors along the propagation axes of the laser beams L_1 and L_2. These axes are tilted respectively from z and x axis by about 5°. Laser intensities are 100 mW/cm^2 for L_1 and 50 mW/cm^2 for L_2 and L_2'. The waist of these beams is 2.8 mm so that the intensity over the condensate is constant. The beams are pulsed on for a duration chosen to maximize the coupling to the $m_x = 0$ state (~ 500 ns).

About 60% of the atoms are transferred in one of the two possible momentum components, forming two superimposed Bose Einstein condensates travelling with a relative velocity of $2v_{\rm rec}$. The center of mass of the collision is in a frame initially travelling upward at one recoil velocity and accelerating downward due to gravity. The recoil velocity is at least 4 times larger than the speed of sound ($v_S = \sqrt{\mu/m}$, μ is the chemical potential) in the initial condensate. This ensures that elementary excitations of the condensate correspond to free particles. The collisions are in the s-wave regime so that the collision products are distributed in velocity space over a spherical shell around the center-of-mass of the two Bose Einstein condensates. We do not switch off the magnetic trap, so that atoms remaining in $m_x = 1$ stay trapped.

After the collision, atoms fall onto a 8 cm microchannel plate (MCP) placed 46.5 cm below the trap center. A delay line anode permits reconstruction of the positions of individual atoms in the $x-y$ plane with an rms resolution width of about 300 μm corresponding to an rms velocity resolution of about $0.01\, v_{\rm rec}$ [28, 31]. The time resolution is 3 ns, giving a vertical position resolution much better than any other relevant length scale in the experiment. An independent measurement of the detection efficiency, averaged over the detector, gives about 10 % [29].

Figure 2 shows successive 2.4 ms time slices showing the atom positions as they cross the detector plane. The time of flight for the center of mass to reach the detector is $t_{\rm TOF} = 320$ ms. At the detector, the collision sphere has a diameter of $2v_{\rm rec}t_{\rm TOF} \sim 5.8$ cm, and is easily visible in Fig. 2. To avoid effects of local saturation of the detector, we exclude regions around the 4 condensates, representing about 40% of the sphere. On the remaining area of the sphere we detect between 30 and 300 atoms on each shot, with an average of about 100 per shot. This means that $\sim 5\%$ of the atoms are scattered from the two condensates. This number is consistent with the expected cross section [35] and the estimated duration of the collision, 200 μs. This duration is the time it takes for the pair production rate to fall by a factor of 4 due to the expansion of the cloud. To estimate this rate, we follow the hydrodynamical approach detailed in Ref. [13].

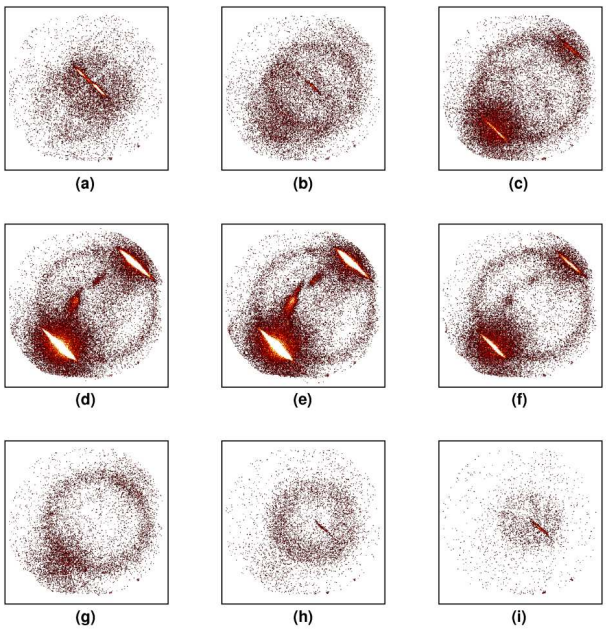

FIG. 2: (Color online) (a-i) Images of the collision of two condensates. Each frame represents a 2.4 ms time slice of the atomic cloud as it passes the plane of the detector ($x-y$). 150 shots have been averaged to obtain these images. The two colliding condensates and the s-wave collision sphere are clearly visible. Other features visible in the images are discussed in the text. The size of each image is 8 cm × 8 cm.

In the mid plane of the sphere one can see the unscattered, pancake-shaped condensates which locally saturate the detector. Other features visible in Fig. 2 include : a condensate which underwent no momentum transfer, frame (a), probably due to the imperfect polarization of a Raman beam which can produce an off resonant Raman transition, a fourth condensate (i) probably resulting from four-wave mixing of the condensate in (a) and the main unscattered condensates [15], and a collision

sphere due to collisions with atoms remaining trapped in $m = 1$ (b). The two spots within the sphere in frames (d) and (e) are not understood.

Knowing the arrival time and position at the detector, we can calculate, for each detected atom, a velocity vector $\mathbf{v}$ in the collision center of mass frame. The collision sphere is a shell with an rms thickness corresponding to a velocity of about $0.08\, v_{\rm rec}$. We expect the shell to be broadened by the uncertainty limit mentioned above. The observed number is close to $v_{yz}^{\rm rms}$, the intrinsic velocity scale for the radial direction. Along the x direction the thickness should be set by $v_x^{\rm rms}$ resulting in an anisotropic shell. The presence of the unscattered condensates however renders the x direction inaccessible. An additionnal broadening mechanism is the acceleration due to the mean field of the condensate. A rough estimate of this effect is found by simply adding the chemical potential to the kinetic energy of a scattered atom. This gives a velocity broadening of order $0.03\, v_{\rm rec}$, which is not entirely negligible compared to $v_{yz}^{\rm rms}$ and shows that mean field effects may be important for both the shell thickness and the correlation function discussed below. In what follows however, we shall neglect any mean field acceleration of the atoms.

To examine the pair correlation function, we construct a three dimensional histogram containing all the pairs with a velocity sum $\mathbf{V} = \mathbf{V_1} + \mathbf{V_2}$ within the set of all the scattered atoms in one shot. We then sum the histograms over 1100 shots. Another histogram containing all the pairs of the sum of all shots gives the accidental coincidence rate for uncorrelated atoms and is used as a normalization. We thus recover the normalized second order correlation function $g^{(2)}(\mathbf{V})$ of the distribution of relative velocities of atom pairs on the s-wave scattering sphere. Figure 3(a) shows the behavior of the projection of $g^{(2)}(\mathbf{V})$ around $\mathbf{V} = \mathbf{0}$ (atoms with opposite velocities) along the three space axes. The peak indicates an increased probability for detecting a pair of atoms of opposite velocities, and is therefore a clear signature of the production of back to back atomic pairs in the scattering process. The peak is clearly anisotropic, and we will discuss the width and height below.

We can also investigate the correlation function for nearly parallel velocities (the HBT effect). Defining the relative velocity $\mathbf{V'} = \mathbf{V_1} - \mathbf{V_2}$ we show in Fig. 3b the correlation function $g^{(2)}(\mathbf{V'})$ around $\mathbf{V'} = \mathbf{0}$. It is evident that the back to back and collinear peaks have very similar shapes.

To analyze these results further, we perform a three-dimensional Gaussian fit to the normalized histograms:

$$g^{(2)}(U_x, U_y, U_z) = 1 + \eta\; e^{-\frac{{U_x}^2}{2{\sigma_x}^2} - \frac{(U_y+U_z)^2}{2{\sigma_{yz}}^2}},$$

with $\mathbf{U} = \mathbf{V}$ for the back to back case (BB) or $\mathbf{U} = \mathbf{V'}$ for the collinear case (CL). The definitions of the widths are slightly different from those of Ref. [28]. Because of the

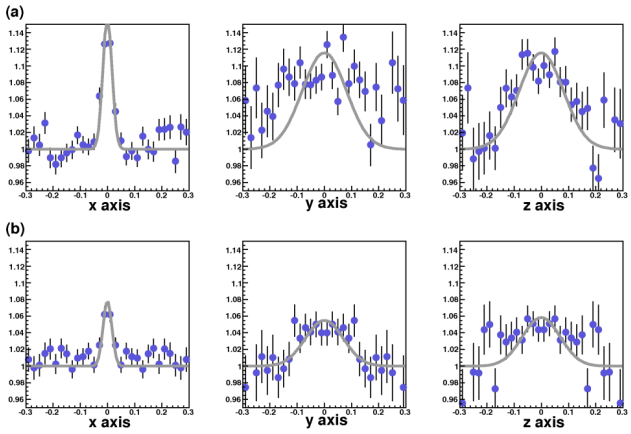

FIG. 3: Back to back (panel a) and collinear (panel b) correlation peaks. (a) Projection of $g^{(2)}(\mathbf{V} = \mathbf{V_1} + \mathbf{V_2})$ along the different axes of the experiment and around $\mathbf{V} = \mathbf{0}$. The projection consists in averaging the correlation in the two other directions over a surface equal to the products of the corresponding correlation lengths. This averaging makes the height smaller than the 3D fitted value $\eta = 0.19 \pm 0.02$. The peak is the signature for correlated atoms with opposite velocities. (b) Projection of $g^{(2)}(\mathbf{V'} = \mathbf{V_1} - \mathbf{V_2})$ along the different axes of the experiment. This peak is due to the Hanbury Brown and Twiss bunching effect.

cylindrical symmetry, we impose identical widths along the y and z axes. In the case of the back to back peak, the fit gives $\eta^{\rm BB} = 0.19 \pm 0.02$, $\sigma_x^{\rm BB} = 0.017 \pm 0.002$ and $\sigma_{yz}^{\rm BB} = 0.081 \pm 0.004$. For the collinear peak we find: $\eta^{\rm CL} = 0.10 \pm 0.02$, $\sigma_x^{\rm CL} = 0.016 \pm 0.003$ and $\sigma_{yz}^{\rm CL} = 0.069 \pm 0.008$. We have expressed the velocity widths in units of the recoil velocity.

In the absence of mean field interactions, which can change the velocity of atoms leaving the condensate, one would expect the rms width of the HBT peak in velocity space to be $v^{\rm rms}/\sqrt{2}$ [32]. In the y and z directions, this naive prediction for the width gives $\sigma_{yz} = v_{yz}^{\rm rms}/\sqrt{2} = 0.064\, v_{\rm rec}$, not too far from the observed values (BB and CL).

In the x direction the width is consistent with the single particle rms detector resolution : the two-particle distribution is $\sqrt{2}$ times larger than the single particle distribution meaning that the rms resolution limit for the correlation function is $\delta = 0.014\, v_{\rm rec}$.

We now turn to the height of the peaks η. In the collinear case we expect the value of η to be unity for a detector resolution much smaller than peak width. Since in the x direction the width is clearly limited by the resolution, a simple estimate for η is the ratio of the ideal width to the observed one: $\eta \approx v_x^{\rm rms}/\sqrt{2}\sigma_x = 0.15$, close to the fitted value.

In the back to back case, the height of the peak is not limited to unity. A simple model of the peak height simply compares the number of true pairs to random coin-

cidences in a volume ΔV defined by the widths observed in Fig. 3 :

$$1+\eta = \frac{\text{true}+\text{random}}{\text{random}} = 1+\frac{V}{N\Delta V} \qquad (1)$$

Here N is the number of atoms scattered on a single shot (but not necessarily detected) and V is the volume of the scattering shell. A rough estimate of $\Delta V/V$ is 1/1400. As mentioned above, we detect on average 100 atoms on the analyzed 60 % of the sphere. Assuming a quantum efficiency of 10 %, a rough estimate of the average number N is 1700 so that we find $\eta \approx 0.8$ which gives the correct order of magnitude. We emphasize that ΔV is limited by the detector resolution in the x direction and is therefore about 10 times larger than the volume corresponding to a single mode. Thus as stated in the introduction, the number of scattered atoms per mode is small compared to unity, and we are in the separated entangled pair production regime. We can verify the $1/N$ dependence of Eq. (1) by binning the data according to the number of scattered atoms per shot. Dividing the 1100 shots into 3 bins of different atom numbers we do observe the expected trend as shown in Fig. 4.

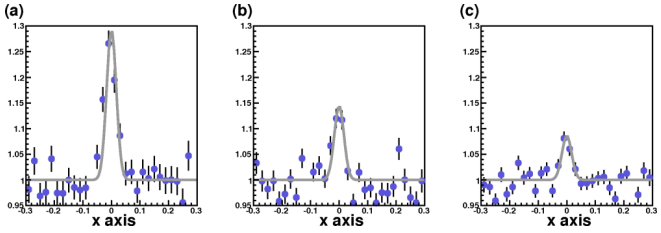

FIG. 4: Projections of $g^{(2)}(\mathbf{V})$ along the x axis and around $\mathbf{V}=\mathbf{0}$. (a) Bin of mean number of detected atoms of 50, (b) of 125 and (c) of 190. As well known in coincidence techniques, increasing the average rate of pairs decreases the contrast of true to accidental coincidences (see Eq. (1)).

Although the data agree qualitatively with a simple model ignoring mean field effects, a more sophisticated description is desirable. Such a description using a quantum stochastic simulation is in progress [36]. Preliminary results show a good agreement between numerical and experimental results.

Having identified a clear pair production process in these collisions, one can also ask about the possibility of observing a sub-Poissonian distribution of the scattered atoms in opposite directions. This investigation is currently in progress. The pair production we have demonstrated here is also a first step toward experiments in which entanglement between atoms in position and momentum might be observed and manipulated [5, 6].

We acknowledge valuable discussions with Karen Kheruntsyan, Klaus Mølmer and Marek Trippenbach. The Atom Optics group of LCFIO is a member of the IFRAF institute, and is supported by the french ANR and by the SCALA programme of the European Union.

* Electronic address: christoph.westbrook@institutoptique.fr

[1] D. C. Burnham and D. L. Weinberg, Phys. Rev. Lett. **25**, 84 (1970).
[2] M. O. Scully and M. S. Zubairy, *Quantum Optics* (Cambridge University Press, Cambridge, UK, 1997).
[3] H. Pu and P. Meystre, Phys. Rev. Lett. **85**, 3987 (2000).
[4] L.-M. Duan, A. Sørensen, J. I. Cirac, and P. Zoller, Phys. Rev. Lett. **85**, 3991 (2000).
[5] K. V. Kheruntsyan, M. K. Olsen, and P. D. Drummond, Phys. Rev. Lett. **95**, 150405 (2005).
[6] T. Opatrný and G. Kurizki, Phys. Rev. Lett. **86**, 3180 (2001).
[7] C. M. Savage, P. E. Schwenn, and K. V. Kheruntsyan, Phys. Rev. A **74**, 033620 (2006).
[8] P. Naidon and F. Masnou-Seeuws, Phys. Rev. A **68**, 033612 (2003).
[9] P. Ziń, J. Chwedeńczuk, and M. Trippenbach, Phys. Rev. A **73**, 033602 (2006).
[10] A. A. Norrie, R. J. Ballagh, and C. W. Gardiner, Phys. Rev. A **73**, 043617 (2006).
[11] P. Ziń *et al.*, Phys. Rev. Lett. **94**, 200401 (2005).
[12] P. Deuar and P. D. Drummond, Phys. Rev. Lett. **98**, 120402 (2007).
[13] Y. B. Band, M. Trippenbach, J. P. Burke, and P. S. Julienne, Phys. Rev. Lett. **84**, 5462 (2000).
[14] A. Heidmann *et al.*, Phys. Rev. Lett. **59**, 2555 (1987).
[15] L. Deng *et al.*, Nature **398**, 218 (1999).
[16] J. M. Vogels, K. Xu, and W. Ketterle, Phys. Rev. Lett. **89**, 020401 (2002).
[17] J. M. Vogels, J. K. Chin, and W. Ketterle, Phys. Rev. Lett. **90**, 030403 (2003).
[18] N. Gemelke *et al.*, Phys. Rev. Lett. **95**, 170404 (2005).
[19] G. K. Campbell *et al.*, Phys. Rev. Lett. **96**, 020406 (2006).
[20] Z. Y. Ou and L. Mandel, Phys. Rev. Lett. **61**, 50 (1988).
[21] Y. H. Shih and C. O. Alley, Phys. Rev. Lett. **61**, 2921 (1988).
[22] A. P. Chikkatur *et al.*, Phys. Rev. Lett. **85**, 483 (2000).
[23] K. Gibble, S. Chang, and R. Legere, Phys. Rev. Lett. **75**, 2666 (1995).
[24] C. Buggle, J. Leonard, W. von Klitzing, and J. T. M. Walraven, Phys. Rev. Lett. **93**, 173202 (2004).
[25] N. R. Thomas, N. Kjærgaard, P. S. Julienne, and A. C. Wilson, Phys. Rev. Lett. **93**, 173201 (2004).
[26] M. Greiner, C. A. Regal, J. T. Stewart, and D. S. Jin, Phys. Rev. Lett. **94**, 110401 (2005).
[27] G. Baym, Act. Phys. Pol. B **29**, 1839 (1998), and references therein.
[28] M. Schellekens *et al.*, Science **310**, 648 (2005).
[29] T. Jeltes *et al.*, Nature **445**, 402 (2007).
[30] A. Robert *et al.*, Science **292**, 461 (2001).
[31] O. Jagutzki *et al.*, Nucl. Inst. & Meth. in Phys. Res. A **477**, 244 (2004).
[32] J. V. Gomes *et al.*, Phys. Rev. A **74**, 053607 (2006).
[33] S. Moal *et al.*, Phys. Rev. Lett. **96**, 023203 (2006).
[34] P. J. Leo, V. Venturi, I. B. Whittingham, and J. F. Babb, Phys. Rev. A **64**, 042710 (2001).
[35] We extrapolate from [33, 34] a value of 5.3 nm for the scattering length between $m=0$ atoms.
[36] A. Perrin, K. Kheruntsyan unpublished